EREM 73/4
Journal of Environmental Research, Engineering and Management
Vol. 73 / No. 4 / 2017
pp. 41-57
DOI 10.5755/j01.erem.73.4.19553

Landform Evaluation through Hypsometric Characterisation: An Example from a Selected River Basin in Southern Western Ghats, India

Received 2017/11 | Accepted after revision 2017/12

crossref http://dx.doi.org/10.5755/j01.erem.73.4.19553

Landform Evaluation through Hypsometric Characterisation: An Example from a Selected River Basin in Southern Western Ghats, India

H. Vijith
Independent Scholar, Formerly affiliated to Department of Applied Geology, Faculty of Engineering and Science Curtin University Malaysia, Malaysia

V. Prasannakumar
Inter University Centre for Geospatial Information Science and Technology, University of Kerala, Kariavattom, Thiruvananthapuram, Kerala, India

P. Pratheesh
Department of Geology, School of Earth Science Systems, Central University of Kerala, Kasaragod, Kerala, India

Corresponding author: vijithh@gmail.com
Independent Scholar, Formerly affiliated to Department of Applied Geology, Faculty of Engineering and Science Curtin University Malaysia, CDT 250, Miri 98009, Sarawak, Malaysia

Characteristics and spatial variation in geomorphic processes in the Meenachil river basin in southern Western Ghats, Kerala, India, is documented by analyzing the hypsometric parameters of 49 subwatersheds of the 5th, 4th and 3rd order. Hypsometric curves and parameters such as hypsometric integral (*Ea*), maximum concavity (*Eh*), coordinates (a*, h*) of the curve-slope inflection point (I), and normalized heights of the hypsometric curve at 20%, 50% and 80% of the area indicate spatial variation. The longitudinal profile of the river shows a highly disturbed region, above a flow length of 20 km and a relatively less disturbed area downstream. The hypsometric integral classifies most of the subwatersheds into mature and mature-to-old age transition while varying shapes of the hypsometric curves imply the influence of tectonic uplift. Variation of hypsometric concavity in

close spatial proximity also confirms the variation in the effect of tectonic processes in the region, where the combination of fluvial and diffusive process is active and are evident from the high hypsometric head and toe measurements. Repeated occurrences of earthquakes in the region confirm the presence of ongoing tectonic activities, which have direct bearing on the geomorphic characteristics of river basin.

Keywords: hypsometry, concavity, landforms, Meenachil, Western Ghats.

Introduction

Morphometric analysis, which reveals the river basin characteristics, usually lacks in-depth details of relief characteristics of the basin. However, detailed analysis of geomorphic evolution history of a drainage basin and its relation to the tectonic uplift is more important in hydrological as well as erosion studies. Comparison of area-elevation data of drainage basins provides detailed information about geomorphic evolutional history and stages of landscape development (Strahler 1952). Critical evaluation of hypsometric (area-altitude) parameters helps to differentiate between tectonically active and inactive areas in a basin (Strahler 1952, Willgoose and Hancock 1998, Singh et al. 2008, Elias 2013), allows a ready comparison of catchments with a diverse area and can characterise the terrain which is influenced by climate, tectonics and lithology (Strahler 1952, Hurtrez et al. 1999, Singh 2009). The hypsometric integral (Ea) indicates the percentage volume of the original basin that remains unaltered and shows the trade-off between erosion and tectonics with respect to the base level erosion (Strahler 1952, Kale and Shejwalkar 2008, Ahmad et al. 2014). Away from this straightforward approach which uses the hypsometric curve shape and integral to understand and classify the geomorphic evolution stage of the drainage basin, Willgoose et al. (1991), Willgoose (1994) and Sinha-Roy (2002) proposed a detailed analysis of hypsometric curve parameters such as hypsometric head, toe, inflection point and concavity. These parameters are used to understand the geomorphic processes, the relative uplift rate of the basin and the classification of landforms. However, very few studies have utilised the characteristics of the hypsometric curve to derive holistic information about the geomorphic evolution stage of river basins (Sinha-Roy 2002, Chattopadhyay et al. 2006, Markose and Jayappa 2011, Gopinath et al. 2014, 2016, Dash et al. 2016).

The Meenachil river basin in the Western Ghats of Kerala, selected for the present study, has witnessed geotectonic activities of various magnitudes possibly affecting the drainage networks and the hydrological regime (Singh et al. 2005, Rajendran et al. 2009). Though the river basin has been subjected to detailed studies to understand basic morphometric characteristics, no attempt has been made to analyse the landform or geomorphic evolution of the basin, particularly using the hypsometric analysis (Vijith and Satheesh 2006, Vincy et al. 2012). Hence, in the present study, an attempt was made to evaluate the landform characteristics of the Meenachil river basin through hypsometric characterisation, with a view to gain insight into the geomorphic evolutional history. In order to achieve the specified aim of the present research, different spatial datasets and analysis tools were used to derive the river basin's hypsometric curve attributes, and are discussed in detail in the methodology section.

Study area

The Meenachil River, originating from the western margin of the Greater Periyar Plateau (GPP), has a channel length of 78 km exhibiting highly undulating topography and drains a total area of 1,272 km^2. This includes high altitude mountain ranges in the east (the Western Ghats), gently undulating rolling plains in the middle and vast alluvial stretch in the river mouth, where the river debouches into the Vembanad estuary (Fig. 1a). The river basin is underlain by hard Precambrian crystalline rocks and recent alluvium. The major rocks present in the area are charnockite, pyroxene granulite, cordierite gneiss, garnet-biotite gneiss, migmatite, granite, laterite, sandstone, and

Fig. 1

Map showing (a) study area location and (b) geology of the river basin with earthquake epicentres

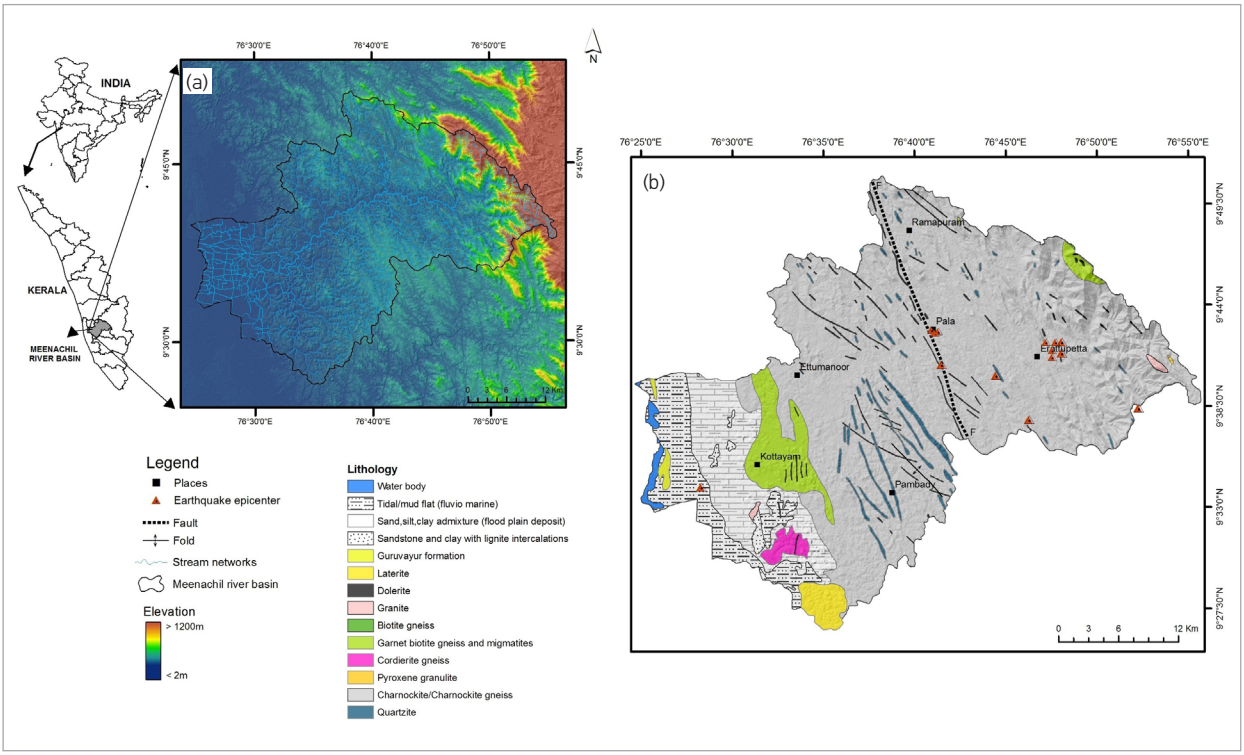

clay with lignite intercalations and recent alluvium (Fig. 1b). Among this, charnockite occupies 72% of the river basin while the other hard crystalline rocks as well as sediments and sedimentary formations cover 21% and 7%, respectively, of the river basin. Dolerite dykes, present in the central and eastern parts of the area follow the prominent direction of lineaments and of faults. The NNW-SSE oriented major fault splits the basin into two, and the region in close proximity to the fault experiences repeated seismic events of magnitude < 5M. The subaerial relief of the basin ranges between < 3m to > 1,200m above the mean sea level. The physiographic classification divides the river basin into lowland (< 8 m), midland (8–75 m) and highland (> 75m). The lowland occupies 11% of the total river basin, whereas the midland and highland cover 57% and 32% of the river basin, respectively. Geomorphology of the region is very complex, varying from the plateau (Peermedu plateau) in the east to the alluvial plains in the western margin. The relative relief of the basin ranges from 2 to 762 m/km^2 with high drainage density of 5,703 m/km^2. The Meenachil river basin receives an annual average rainfall > 3,000 mm and the river has a total annual yield of 2,349 million cm^3.

Materials and methods

Assessment of terrain evolution through characterisation of watershed has attained more importance in recent time through a wide application of Geographical Information System (GIS) and Digital Elevation Model (DEM) data. In order to characterise the geomorphic evolution of the Meenachil river basin, moderate resolution Shuttle Radar Topographic Mission (SRTM) digital elevation data, available on the USGS website (http://earthexplorer.usgs.gov/), were downloaded and processed. SRTM data with 30-m ground resolution offer better accuracy with very few voids and artefacts. DEM downloaded for the present study

also contains very few voids and is filled by a running void filling tool available in ArcGIS software. Using the void-fill processed DEM in ArcHydro extension, watershed and drainage networks were derived. Drainage networks derived are ordered, based on the Strahler's (1952) system, and the river basin is further divided into 49 subwatersheds of various orders (Fig. 2). Among these, 9 are 5th order, 27 are 4th order and 13 subwatersheds come under 3rd order. Before proceeding to the subwatershed-based detailed analysis, a longitudinal profile of the major river was generated by sampling the elevation at a unique distance of 250 m from its origin, in order to identify and understand the geomorphic evolution and geological processes operating in the basin.

The digital elevation model data were subsetted using the subwatershed boundaries and were taken to the SAGA 2.1.2 software for the generation of a hypsometric table for further analysis and interpretation. The normalised area-elevation (hypsometric) table, thus derived, was used to generate the hypsometric curve and the hypsometric integral (area under the hypsometric curve) using the statistical software GraphPad Prism 5. The hypsometric curve was characterised through the methodology proposed by Sinha-Roy (2002) and basic parameters shown in Figure 3 were generated. Parameters derived from hypsometric curves are hypsometric integral (*Ea*), maximum concavity (*Eh*), coordinates (a*, h*) of the curve-slope inflection point (I) and normalised heights of the

Fig. 2

Map showing 49 subwatersheds considered in the present analysis

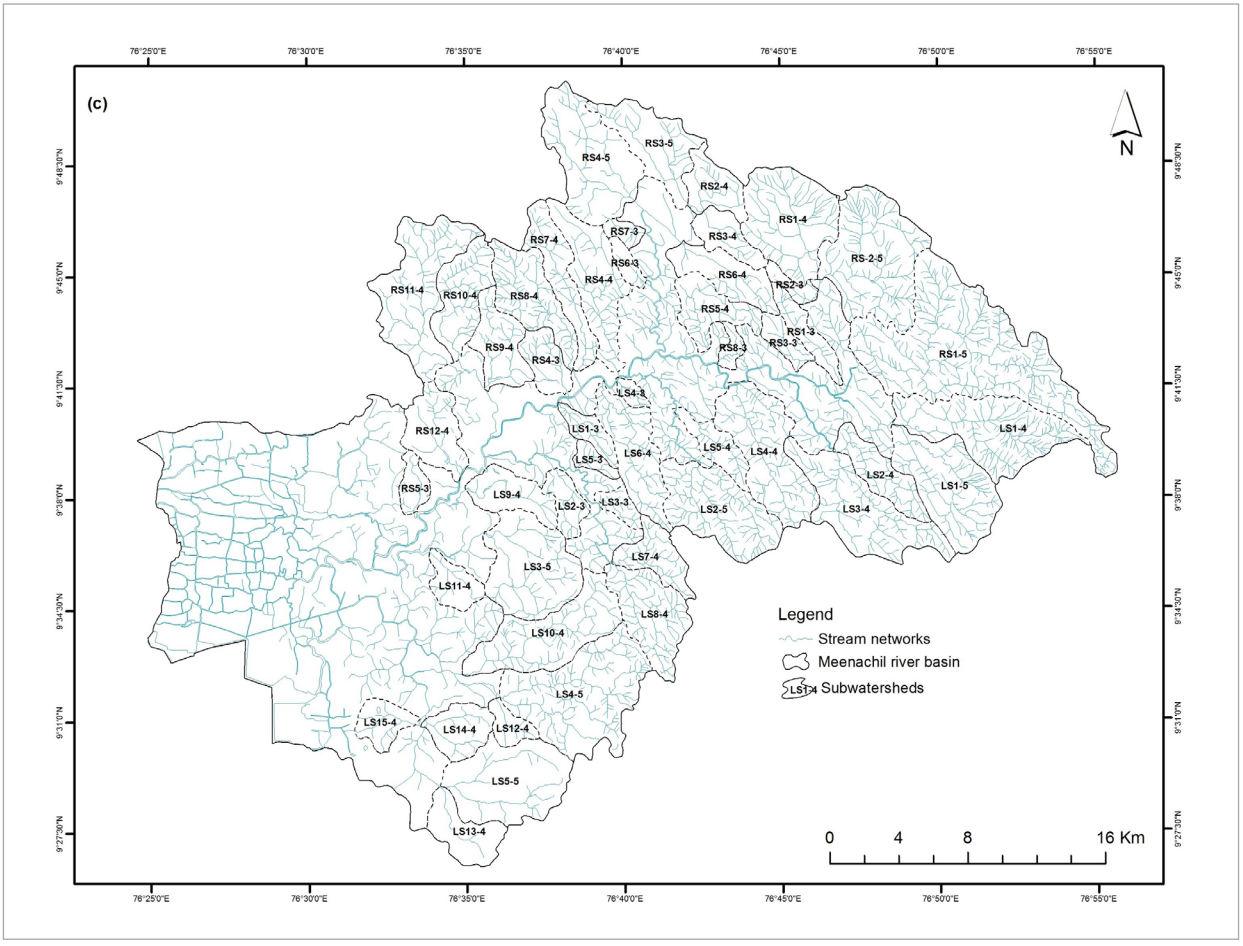

hypsometric curve at 20%, 50% and 80% of the area (h (0.2), (0.5), (0.8)).

Fig. 3

Hypothetical hypsometric curve used to derive hypsometric parameters (modified after Sinha-Roy, 2002)

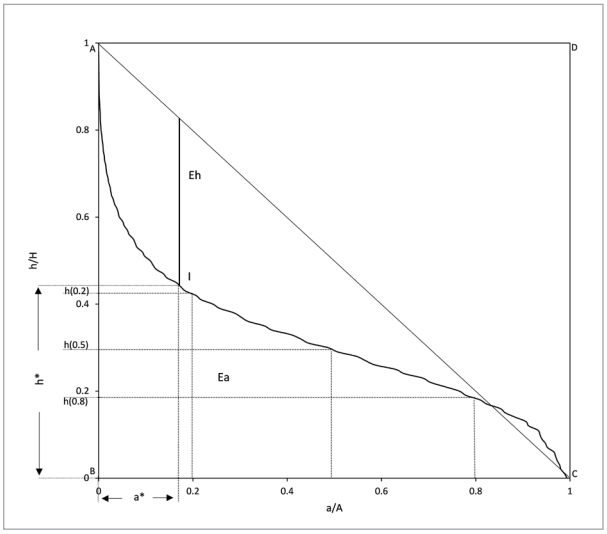

Morphometric parameters related to erosion and terrain evolution, such as drainage density (D_d), relative relief (R_r) and dissection index (DI) of each subwatershed, were calculated to assist the interpretation of terrain evolution through hypsometric characterisation. Drainage density is calculated by dividing the total length of drainages by the subwatershed area (Horton 1945) and the relative relief was assessed by dividing the maximum basin relief (H) with the perimeter of the basin (L_b) (Melton 1957). The dissection index (DI) of an individual subwatershed was calculated based on the methodology proposed by Nir (1957) by dividing the relative relief (R_r) with the absolute relief of the basin (A_r). The absolute relief (A_r) of each subwatershed was calculated by measuring the maximum height of the subwatershed from DEM.

Results

The longitudinal profile of the Meenachil River was generated using the elevation points, sampled at the unique distance shown in Figure 4. The elevation-distance graph shows variable characteristics of profiles at a different flow distance from its origin point. In general, the high elevated upper catchment region shows convexity in the channel profile, followed by concavity and then smooth graded nature. The results of all the morphometric and hypsometric parameters derived are shown in Table 1 and are discussed in detail below. The subwatersheds of the Meenachil river basin consist of 5th, 4th and 3rd orders having a different dimension and relief. The area of the 5th order subwatersheds ranges from 17 to 68 km^2, which is found to be occurring more in the upper catchment region

Fig. 4

Longitudinal profile of the Meenachil River showing variation in channel characteristics

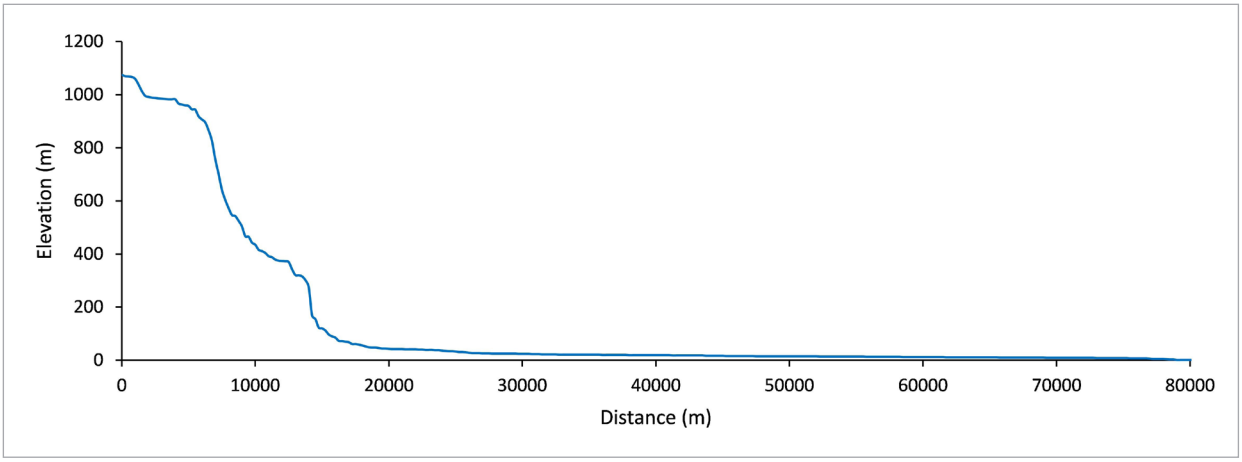

Table 1

Morphometric and hypsometric parameters of 49 subwatersheds considered in the study

							Coordinates of I		Height of curve at		
Subwatershed name	Area (km²)	Dd	Rr	DI	Ea	Eh	a*	h*	0.2	0.5	0.8
LS1-5	26.35	1.9	3.73	0.42	0.22	0.42	0.2	0.39	0.39	0.16	0.04
LS2-5	25.18	2.6	0.93	0.38	0.29	0.46	0.1	0.44	0.4	0.29	0.17
LS3-5	26.67	2.7	0.62	0.44	0.27	0.4	0.2	0.4	0.4	0.24	0.11
LS4-5	38.82	2.6	0.45	0.29	0.31	0.38	0.2	0.42	0.42	0.29	0.18
LS5-5	28.22	2.8	0.45	0.41	0.34	0.35	0.16	0.5	0.48	0.35	0.18
RS1-5	68.72	2.1	2.11	0.18	0.37	0.18	0.5	0.32	0.65	0.29	0.06
RS2-5	35.37	2.0	3.66	0.33	0.34	0.22	0.15	0.63	0.6	0.31	0.09
RS3-5	17.42	2.3	1.92	0.38	0.16	0.51	0.3	0.19	0.33	0.08	0.01
RS4-5	28.78	2.6	1.29	0.35	0.11	0.64	0.16	0.2	0.17	0.09	0.01
LS1-4	30.4	1.9	3.78	0.32	0.31	0.21	0.3	0.39	0.52	0.25	0.07
LS2-4	11.38	2.3	1.85	0.50	0.25	0.39	0.1	0.51	0.41	0.2	0.09
LS3-4	27.80	2.3	1.28	0.30	0.22	0.47	0.3	0.23	0.42	0.11	0.04
LS4-4	26.52	2.6	0.69	0.34	0.17	0.53	0.1	0.37	0.28	0.15	0.05
LS5-4	7.28	2.9	0.49	0.47	0.31	0.42	0.19	0.39	0.39	0.28	0.21
LS6-4	17.52	2.7	0.65	0.38	0.39	0.22	0.1	0.68	0.6	0.4	0.16
LS7-4	9.76	2.7	0.80	0.45	0.49	0.15	0.1	0.75	0.67	0.47	0.34
LS8-4	18.62	2.7	0.56	0.35	0.35	0.33	0.14	0.53	0.49	0.33	0.2
LS9-4	10.57	2.6	0.63	0.58	0.22	0.4	0.29	0.31	0.42	0.15	0.01
LS10-4	26.04	2.6	0.49	0.35	0.33	0.29	0.1	0.61	0.51	0.29	0.16
LS11-4	6.76	2.8	0.62	0.76	0.27	0.34	0.17	0.5	0.46	0.23	0.05
LS12-4	4.49	3.0	0.68	0.85	0.38	0.24	0.2	0.56	0.56	0.35	0.19
LS13-4	11.10	2.9	0.46	0.60	0.35	0.34	0.1	0.55	0.48	0.34	0.21
LS14-4	9.54	2.5	0.63	0.76	0.36	0.25	0.2	0.54	0.54	0.34	0.17
LS15-4	6.84	2.8	0.39	0.82	0.45	0.13	0.1	0.76	0.68	0.45	0.24
RS1-4	27.30	2.4	3.48	0.43	0.17	0.52	0.2	0.28	0.28	0.1	0.03
RS2-4	9.43	2.3	2.97	0.58	0.22	0.45	0.1	0.45	0.38	0.19	0.04
RS3-4	7.64	2.4	1.88	0.63	0.18	0.53	0.2	0.27	0.27	0.1	0.03
RS4-4	19.71	2.4	0.92	0.35	0.22	0.47	0.19	0.34	0.33	0.17	0.06
RS5-4	11.49	2.8	0.83	0.48	0.31	0.41	0.2	0.39	0.39	0.28	0.22
RS6-4	12.62	2.5	1.27	0.45	0.14	0.58	0.1	0.32	0.23	0.11	0.02
RS7-4	13.73	2.5	0.79	0.37	0.24	0.43	0.2	0.37	0.37	0.19	0.07
RS8-4	17.52	2.6	0.57	0.39	0.3	0.34	0.17	0.5	0.47	0.26	0.11
RS9-4	12.46	2.4	0.78	0.50	0.31	0.28	0.2	0.52	0.52	0.28	0.09
RS10-4	15.41	2.6	0.67	0.46	0.38	0.2	0.2	0.6	0.6	0.35	0.16
RS11-4	29.39	2.6	0.36	0.28	0.3	0.34	0.2	0.46	0.46	0.27	0.12
RS12-4	13.33	2.9	0.71	0.54	0.19	0.51	0.2	0.29	0.29	0.13	0.04
LS1-3	4.97	2.5	0.91	0.74	0.51	0.14	0.1	0.76	0.69	0.53	0.35
LS2-3	6.18	2.8	0.87	0.71	0.35	0.25	0.1	0.65	0.56	0.35	0.13
LS3-3	3.55	2.6	1.50	0.90	0.36	0.25	0.1	0.65	0.56	0.32	0.18
LS4-3	2.10	3.0	1.05	1.22	0.38	0.57	0.1	0.33	0.27	0.16	0.02
LS5-3	2.89	2.6	1.26	0.98	0.38	0.16	0.2	0.64	0.64	0.38	0.1
RS1-3	6.81	2.4	1.44	0.57	0.26	0.36	0.2	0.44	0.44	0.19	0.06
RS2-3	3.02	2.5	3.15	0.92	0.38	0.21	0.04	0.76	0.67	0.37	0.08
RS3-3	4.78	2.4	1.19	0.80	0.32	0.3	0.3	0.4	0.52	0.27	0.15
RS4-3	7.79	2.4	0.86	0.72	0.23	0.44	0.2	0.36	0.36	0.19	0.05
RS5-3	4.48	3.0	0.47	0.83	0.21	0.39	0.2	0.4	0.4	0.13	0.01
RS6-3	2.97	2.2	2.39	1.06	0.26	0.5	0.3	0.3	0.4	0.2	0.07
RS7-3	2.53	2.5	2.73	1.20	0.23	0.44	0.2	0.36	0.36	0.16	0.05
RS8-3	2.54	2.4	1.74	1.03	0.25	0.37	0.3	0.33	0.44	0.19	0.05

**Dd – drainage density; Rr – relative relief; DI – dissection index; Ea – hypsometric integral; Eh – concavity; a*, h* – coordinates of the curve-slope inflection point (I); 0.2, 0.5, 0.8 – normalised heights of the hypsometric curve at 20%, 50% and 80% of the area.

than the middle and lower reach of the river basin. The 4th order subwatersheds, having the area between 4 to 30 km^2, are spatially distributed in the river basin. At the same time, the 3rd order subwatersheds show minimal distribution in upper and middle reaches of the basin with the area ranging from 2 to 7 km^2. The shape of subwatersheds varies from circular/semi-circular to elongate, irrespective of the location of subwatersheds. Morphometric parameters such as drainage density (D_d), relative relief (R_r), and dissection index (DI) show variation among the same order of subwatersheds. Drainage density of the 5th order subwatersheds ranges from 1.9 to 2.7 km/km^2, whereas that of the 4th and the 3rd order subwatersheds varies between 1.8 to 3 km/km^2 and 2.2 to 3.7 m/km^2, respectively. The relative relief of the subwatersheds shows a larger difference in all subwatersheds irrespective of its order and size and varies between 0.45 to 3.7, 0.3 to 3.7 and 0.4 to 3.1, respectively, for the 5th, the 4th and the 3rd order subwatersheds. The dissection index (DI) of the subwatersheds varies widely from the 5th to the 3rd order. The dissection index assessed for the 5th order subwatersheds ranges from 0.18 to 0.44, whereas the 4th and the 3rd order subwatersheds show higher values, such as 0.82 and 1.22, respectively, within the range of 0.28 to 0.85 and 0.71 to 1.22. The varying values of drainage density, the relative relief and the dissection index are closely related to lithology.

The hypsometric curve and the integral (*Ea*), generated for the subwatersheds, show different (shape) characteristics with a varying range of hypsometric integrals. While comparing with standard hypsometric curves proposed by Strahler (1956), the hypsometric curves of different orders of the subwatersheds show concave as well as convex shapes (Fig. 5). Among the 5th order subwatersheds, LS1-5, RS3-5 and RS4-5 are concave in shape, whereas all others are convex. At the same time, the subwatersheds that are concave in nature possess low *Ea* (< 0.25). The subwatersheds show convexity and the *Ea* ranges from 0.27 to 0.37. In the case of twenty-seven 4th order subwatersheds, the *Ea* ranges from 0.14 to 0.49. Among this, 12 subwatersheds show *Ea* < 0.30 with a concave curve and the remaining 15 subwatersheds have *Ea* > 0.30 and show concave-convex curves. A similar trend was also noted in the 3rd order group of the subwatersheds. Among this, 6 subwatersheds possess *Ea* < 0.30 with concave curves

Fig. 5

Hypsometric curves of subwatersheds: (a) 5th order, (b) 4th order, and (c) 3rd order

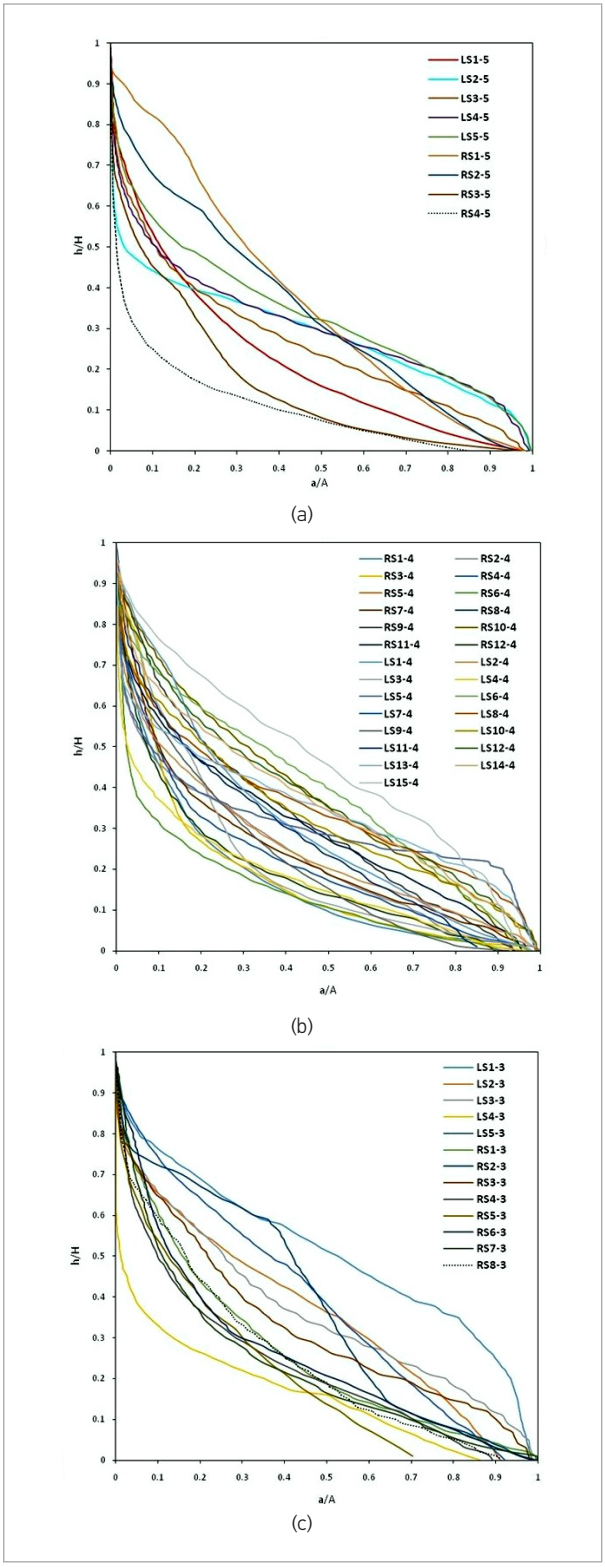

Fig. 6

Landform models developed based on hypsometric curve shapes (modified after Troeh, 1965, and Sinha-Roy, 2002)

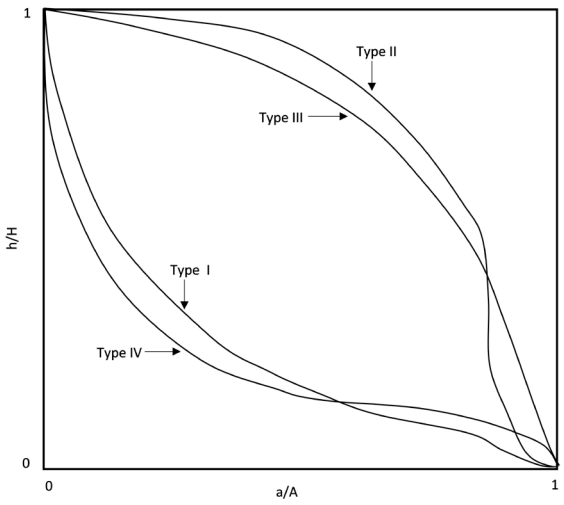

and all others show variable convexity with *Ea* > 0.30.

The landform evolution model proposed by Troeh (1965) and widely discussed by Willgoose et al. (1991) and Willgoose (1994) categorises subwatersheds into 2 distinct types, i. e. Type-I and Type-IV, based on the shape of the hypsometric curve (Fig. 6). The shape of the hypsometric curve reflects the dominant landform process operated in the study area. Subwatersheds having hypsometric curves resembling to Type-I standard curve indicate the dominance of fluvial processes whereas those with Type-IV characteristics suggest the earlier stages of fluvial processes and later episodes of diffusive processes in the lower catchment region or mass accumulation in the downstream, which caused an increase of elevation in the catchment mouth. Among the 49 subwatersheds, 29 subwatersheds come under Type-I and the remaining 20 fall in Type-IV class. Five of the 5th order subwatersheds show Type-I curve characteristics while the remaining ones show Type-IV characteristics. In the case of the 4th order subwatersheds, 14 show Type-I and 12 show Type-IV curve characteristics. At the same time, the majority (9 subwatersheds) of the 3rd order subwatersheds are Type-I class and only 4 subwatersheds show Type-IV curve characteristics (Fig. 7).

Concavity (Eh) of the hypsometric curve, measured at the maximum slope inflection point (I) of the curve with respect to a straight line connecting the head and toe of the hypsometric curve varies from 0.18 to 0.51 for 5th order and 0.13 to 0.58 for the 4th order subwatersheds. At the same time, the 3rd order subwatersheds show the minimum concavity of 0.14 and the maximum of 0.57, reflecting the variation in shape characteristics of the hypsometric curves. Generation of the normalised hypsometric curve and derivation of the hypsometric curve height (h) at defined intervals of the normalised area (a) 0.20, 0.50 and 0.80 indicate highly variable characteristics among the subwatersheds. The hypsometric curve-head height, measured at the point *h (0.20),* varies from 0.17 to 0.69, but the majority of the subwatersheds show a value < 0.50. Among the 5th order subwatersheds, *h (0.20)* varies from 0.17 to 0.65, whereas in the 4th order subwatersheds, it is 0.23 to 0.68. The highest *h (0.20)* value of 0.69 is observed in the 3rd order subwatershed (LS1-3) and the values vary from the lowest value of 0.27 (LS4-3). At the same time, in the case of the hypsometric toe height measured at the point *h (0.80),* the lower order subwatersheds are found to show relatively higher values. In the 5th order subwatersheds, *h (0.80)* varies from 0.01 to 0.18, whereas in the 3rd order subwatersheds, it is between 0.01 and 0.34. A similar high value (0.55) is observed in the 3rd order subwatersheds with the lowest value as 0.01.

Fig. 7

Classification of subwatersheds based on landform process: (1) Type I landform, and (2) Type IV landform

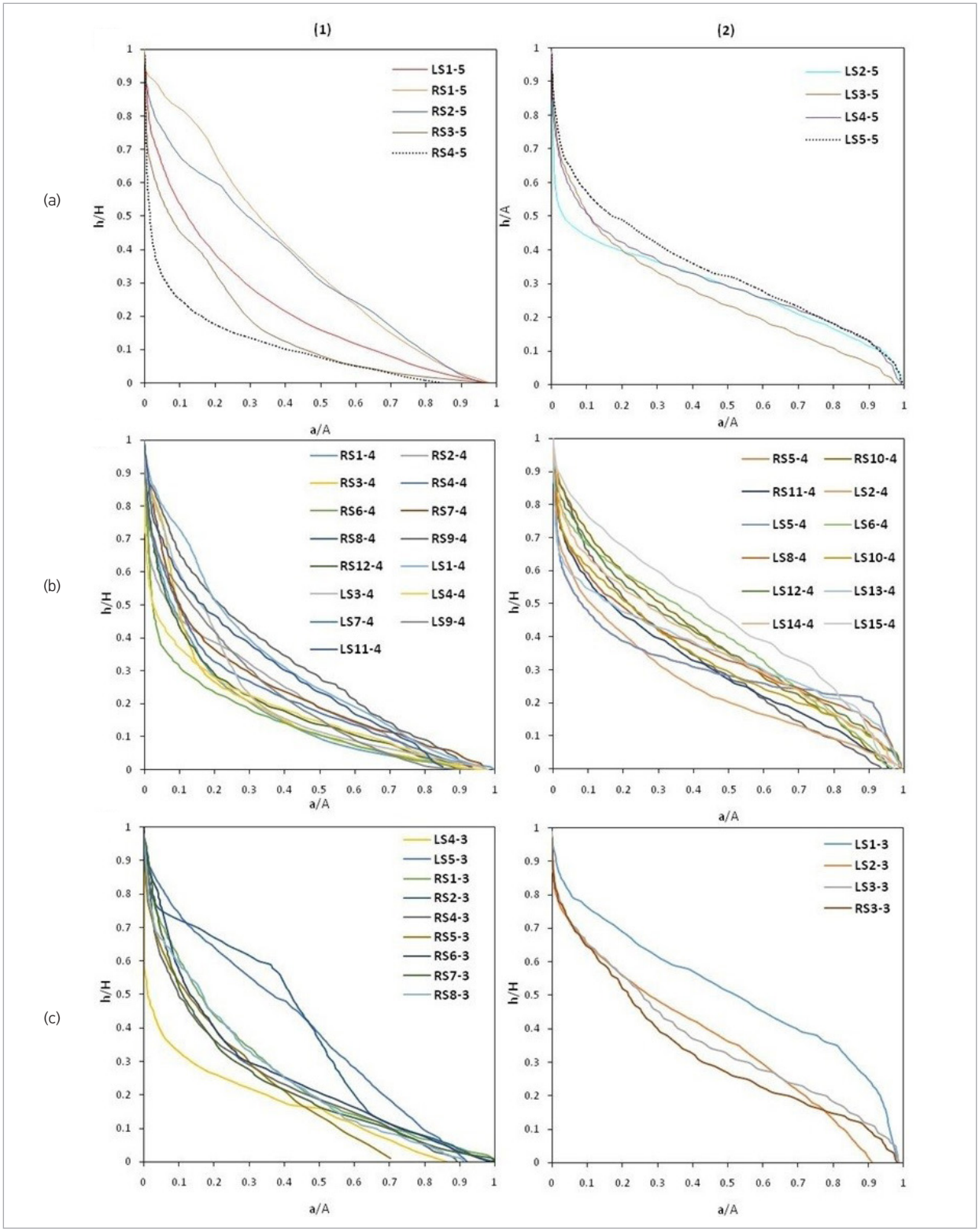

Discussion

The longitudinal profile of the stream is the transient expression of fluvial processes, reflecting geological influences such as available relief, tectonic history, base level change, process of erosion, deposition and of the distribution of outcrops of different lithology (Horton 1945, Strahler 1952, Gardner 1983, Hancock et al. 1998, Trevisani et al. 2010, Castillo 2017). The longitudinal profile of the Meenachil River shows steep slopes with a convex profile and intermittent flat segments up to a flow distance of 20 km from its origin. The variation in the general trend is marked by various kinds and sizes of waterfalls and rapids, which can be considered as knick points where the basement rock is exposed. After the flow length of 20 km, the Meenachil River reaches an elevation < 80 m and flows westerly with a smooth graded profile showing very little change in gradient. Concave, convex and combination (concave-convex) profiles, representing the effect of factors like lithological variation, increased discharge/stream action and tectonics, will help to differentiate the prominent factor responsible for shaping the stream bed and channel characteristics. An abrupt change in channel longitudinal profile characteristics indicates geological control over the stream segment. Profile characteristic variation above and below the flow distance of 20 km from the origin of the river splits the basin into 2 segments. This division is well evidenced through the presence of major faults/lineaments cross cutting the river basin. The river that flows through the upper segment region shows the maximum variation in the stream profile and presence of rapids and waterfalls of various dimensions. Recent occurrence of seismic events in the upper segment region of the river basin indicates a relatively higher effect of the tectonic process in the upper segment than the lower. The characteristic shape of the longitudinal profile nullifies the effect of lithological variation in causing such changes, because the river flows through a single (uniform) lithology (hard crystalline rock) for most of its flow length suggesting a differential effect of the tectonic process in the region. This is supported by the spatial variation in the morphometric parameters in subwatersheds with unique and uniform lithology.

Comparison of the area, drainage density, relative relief and the dissection index with the hypsometric integral (*Ea*) of each subwatershed was carried out to understand the relationship between watershed parameters and hypsometric characters (Fig. 8). The area of subwatersheds and *Ea* show varying relationship in different orders. The 5th order subwatersheds, which cover a large area, show a positive correlation with *Ea,* i. e., if the area increases, the *Ea* also increases (r = 0.60), whereas the 4th and the 3rd order subwatersheds show a weak negative correlation (r = -0.24 and r = -0.14) with no consistent relationship. At the same time, it is also noted that some subwatersheds with a lower area possess high *Ea*. This indicates less erosion in subwatersheds compared with others that possess a large area and a relatively high runoff. Comparison of *Ea* with drainage density, relative relief and the dissection index shows a positive and a negative correlation. Drainage density of a subwatershed depends on the area and the total length of drainages in that area, which indirectly gives the clues to the erosional characteristics of the region. Drainage density of the 5th order subwatersheds shows a negative correlation (r = -0.14), whereas the 4th order subwatersheds show a positive correlation (r = 0.37) with *Ea*. A similar trend with a positive correlation is also noted in the 3rd order subwatersheds (r = 0.17), but with local clustering. Though the drainage density shows variations among the subwatersheds, comparatively high drainage density in a few subwatersheds indicates high erosion from the region. This is supported by the negative correlation observed in higher order subwatersheds. The hypsometric integral and relative relief of the subwatersheds show a negative correlation irrespective of the subwatershed order. Among this, the 5th order subwatersheds show a distinct characteristic than the other two orders of the subwatersheds (r = -0.004). The correlation shown by the 4th and the 3rd order subwatersheds is -0.38 and -0.09, respectively. The higher elevation subwatersheds show a comparatively higher relative relief and lower *Ea*, whereas the lower elevation subwatersheds show high *Ea* and a low relative relief and indicate high rates of the denudation

Fig. 8

Linear plot showing the relationship between hypsometric integral against area, drainage density, relative relief and dissection index: (a) 5th, (b) 4th, and (c) 3rd order subwatersheds

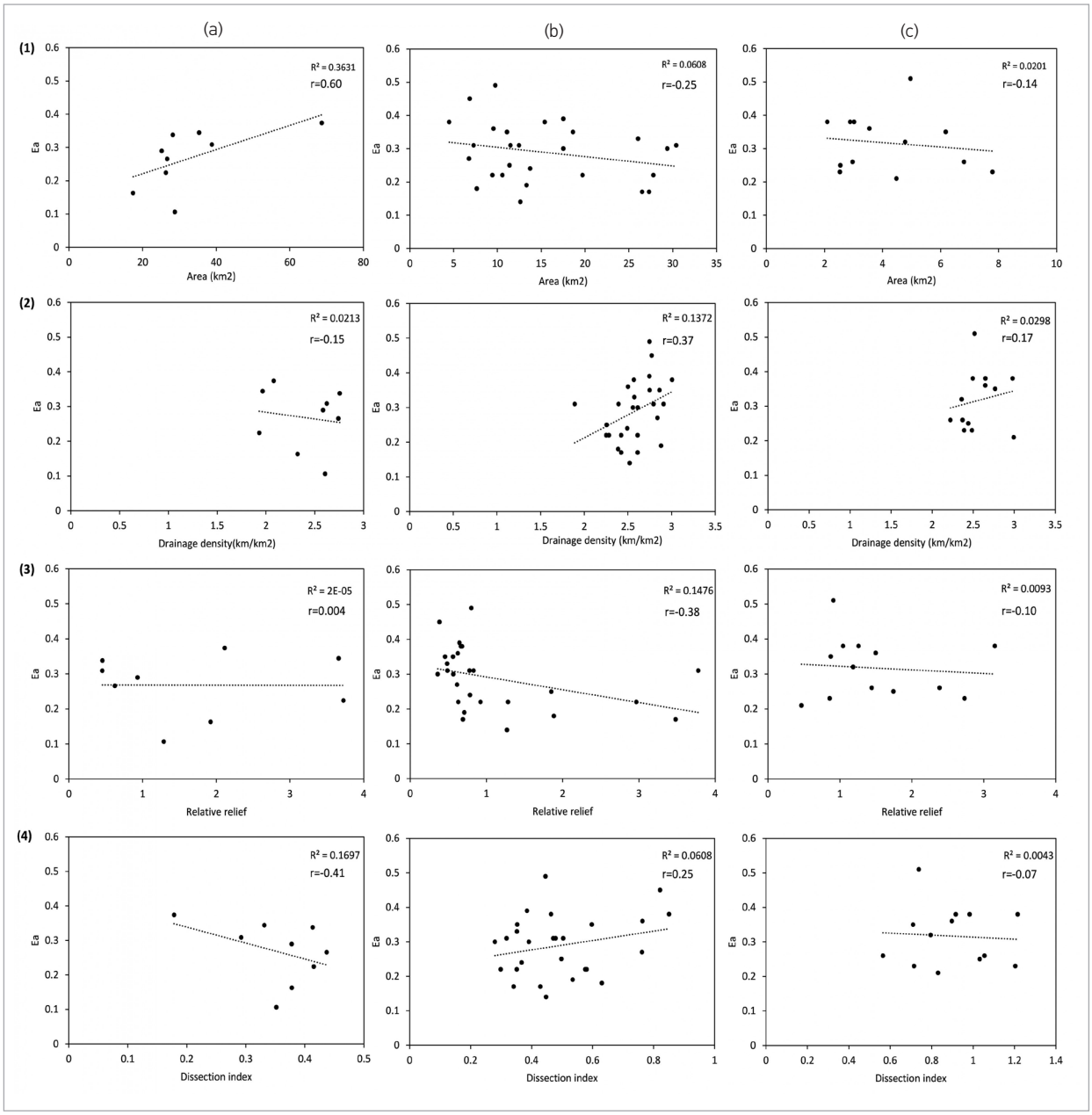

process in the upper catchment region. The *Ea* and the dissection index show alternating negative and positive correlations for the respective orders of subwatersheds. The 5th order subwatersheds show a correlation of -0.41, whereas the 4th order subwatersheds show a positive correlation (r = 0.24). At the same time, the 3rd order subwatersheds show a weak negative correlation (no correlation r = -0.06). All these indicate the differential structural complexity of the subwatersheds in close spatial proximity.

The hypsometric integral (*Ea*) and the shape of hypsometric curves are capable of revealing the geomorphic evolutional stage and the dominant denudation process operating in the subwatershed. Though the subwatersheds of different orders show varying *Ea* and hypsometric curves, the majority of the subwatersheds (28 numbers) possess *Ea* ≥ 0.30, indicating a mature geomorphic evolutional stage. The remaining 21 subwatersheds with *Ea* < 0.30 correspond to the old age stage of geomorphic evolution. At the same time, the characteristic concave upward pattern of the hypsometric curve, inherent of old age landforms, is not perfectly seen in the subwatersheds having *Ea* < 0.30. Most hypsometric curves show a combination of concave-convex shape. This indicates the dominance of geological processes rather than fluvial processes in the region and its influence over base level changes associated with uplift. On the contrary, subwatersheds categorised as in the mature stage of their geomorphic evolution show varying convexity with a threshold in the toe portion of the curve. The shape of the hypsometric curve, especially the head and toe, will assist to differentiate the landform (denudation) process operating in the area. The subwatersheds with absolute concave hypsometric curves indicate the dominance of the fluvial erosional process and those having a convex head and toe indicate the coupled effect of fluvial and diffusive processes in the catchment. The subwatersheds of the Meenachil river basin predominantly show 2 major hypsometric curve shapes corresponding to Type-I and Type-IV curves proposed by Troeh (1965) suggesting variation in landform processes operating in the near neighbourhood, such as fluvial processes and later episodes of diffusive processes in the lower catchment region or mass accumulation in the lower parts of the subwatersheds. Though the subwatersheds have more or less similar lithology, while considering the spatial occurrence of the subwatersheds, it is noted that the majority of the right bank subwatersheds are Type-I whereas those on the left bank belong to Type-IV landform processes.

A direct relationship exists between the shape of the hypsometric curve and its concavity. The measure of concavity (*Eh*) directly indicates the terrain condition in terms of erosivity or the area remaining to be eroded. If the hypsometric curve is close to the ordinate axis, the region is in the old age stage of its geomorphic evolution and possesses high concavity (*Eh*) and a low hypsometric integral (Fig. 9). In the Meenachil river basin, the Eh of the 5th, the 4th and the 3rd order subwatersheds shows a higher negative correlation (r = -0.91, -0.94 and -0.62, respectively) with *Ea*. Though the correlation shown by the 3rd order group of subwatersheds is relatively high, the majority of the subwatersheds fall in the mature or mature-to-old age transition stage of geomorphic evolution. Similarly, the subwatersheds indicating high concavity suggest the transition of the terrain to the old age stage or in the peneplanation stage of terrain evolution (Sinha-Roy 2002, Dash et al. 2016). An inverse relationship is noted with concavity (*Eh*) and the area of the 5th and the 3rd order subwatersheds (-0.69 and -0.13), whereas a weak positive correlation (r = 0.14) exists for the 4th order subwatersheds. *Eh* is higher in the subwatersheds belonging to Type-I curve than those of the Type-IV curves. The results of the present study, consistent with those by Sinha-Roy (2002), suggest that watersheds with higher areas possess less incision and were controlled by the altitude distribution of the subwatersheds.

Measurements of the slope inflection point (I) and its x, y coordinates *a** and *h** derived from the hypsometric curves substantiate the evidences of geomorphic evolution of subwatersheds along with hypsometric integral and concavity. The *a** derived for the subwatersheds varies between 0.04 to 0.5, whereas *h** ranges from 0.19 to 0.46. It is also noted that high *a** and *h** values correspond to subwatersheds belonging to the mature stage of geomorphic evolution (*Ea* > 0.30), whereas the higher *a** and lower *h** indicate the old age (*Ea* < 0.30) stage of subwatersheds. This relationship is well explained in the scatter plot of *a** against *h**, which shows clusters indicating 2 different relationships as discussed (Fig. *9*). It gives an inverse correlation between *a** and *h** (-0.41, -0.56 and -0.72, respectively, for the 5th, the 4th and the 3rd order subwatersheds). Sinha-Roy (2002) suggested that the increase of *a** corresponds to *h** indicating the dominance of diffusive (slope dominated) processes whereas the lower *h** and higher *a** indicate the importance of the fluvial process in landform evolution.

Fig. 9

Linear plot showing the relationship between hypsometric integral against concavity, area, a* and h*: (a) 5th, (b) 4th, and (c) 3rd order subwatersheds

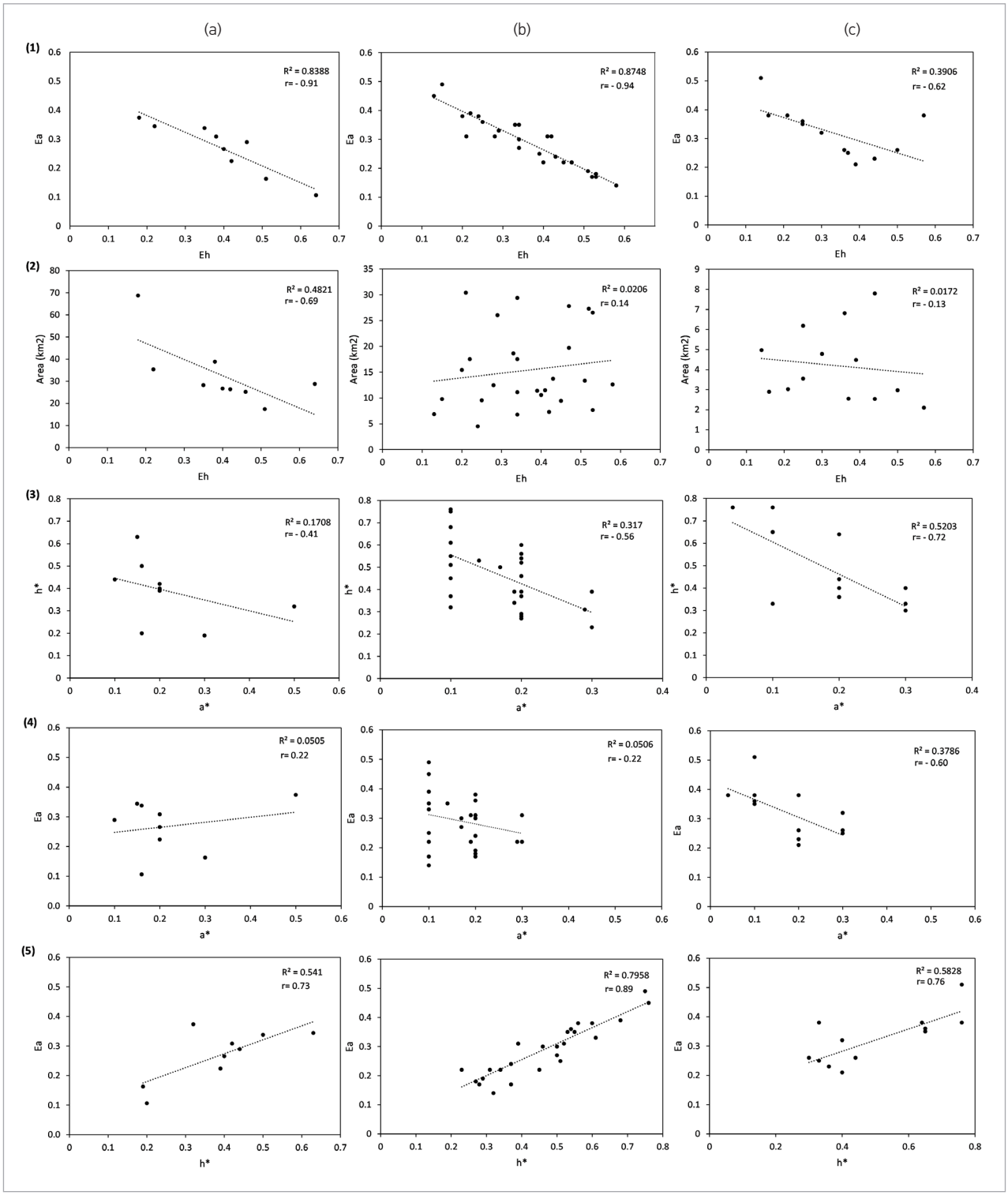

In general, the relationship between Ea, *a** and *h** can be used to classify subwatersheds on the basis of the geomorphic evolutional stage. High *a** and *h** return higher *Ea* (represent mature or youthful topography) and lower *a** and *h** return lower *Ea* (old age topography). However, in the present study, the *a** and *h** show a varying correlation with *Ea*. In the case of *Ea* and *a**, the 5th order subwatersheds are positively correlated indicating the dominance of diffusive processes in the subwatersheds whereas the other subwatersheds (4th and 3rd order) show an inverse relationship. The subwatersheds which show an inverse relationship between *Ea* and *a** suggest mass accumulation of material, in the middle and lower reaches of the subwatersheds, derived from the dominant hillslope processes (Sinha-Roy 2002). At the same time, *Ea* and *h** of all the subwatersheds show a positive correlation.

The dominant geomorphic process of the study area can be assessed through the analysis of hypsometric head *h(0.20)*, body *h(0.50)* and toe *h(0.80)* values, which are capable of differentiating the effect of fluvial and diffusive processes operating in the study area. The high value of the hypsometric head (*h(0.20)*) indicates the dominance of diffusive (slope) processes, whereas the higher value of the hypsometric toe (*h(0.80)*) reflects the influence of the fluvial process and deposition of mass wasting products in the lower part of subwatersheds (Sinha-Roy 2002). In the Meenachil river basin, the 5th order subwatersheds (LS1-5, RS1-5, RS2-5, RS3-5 and RS4-5) show a higher hypsometric head value with an average of *h(0.20)* = 0.42, indicating the relative importance of the diffusive process. At the same time, subwatersheds LS2-5, LS3-5, LS4-5 and LS5-5 show higher hypsometric toe values (average *h(0.80)* = 0.16) suggesting mass accumulation in the downstream or the mouth portion of the river basin. A similar trend is observed among 4th and 3rd order groups of subwatersheds, which show high hypsometric heads (*h(0.20)* = 0.44 and 0.48) indicating the dominance of the slope process rather than the fluvial process in the terrain evolution. Though all the subwatersheds show dominance of the slope process in the headwater regions, the subwatersheds belonging to the 4th order (LS5-4, LS-6-4, LS7-4, LS8-4, LS10-4, LS12-4, LS13-4, LS15-4, RS5-4, RS8-4, RS10-4 and RS11-4) and 3rd order (LS1-3, LS2-3, LS3-3 and RS3-3) show a relatively higher hypsometric toe (*h(0.80)* > 0.10), suggesting the combined effect of fluvial and diffusive mass wasting processes in landscape evolution. The maximum hypsometric curve height at *h(0.20)* was seen in Type-IV curves rather than Type-I. A similar trend is observed in hypsometric body *h(0.50)* and toe *h(0.80)* heights measured. Subwatersheds come under Type-I class showing a low hypsometric toe value than those under Type-IV. This indicates the combined action of the slope-dominated headwater process and the fluvial dominated mass accumulation in the downstream segment in later stages of subwatershed evolution. Upper catchment regions of the Meenachil River undergo severe mass wasting through landslides and soil erosion, reflected as the high value at *h(0.20)*, leading to increased accumulation of slope-derived debris in the lower portion of the river basin or the confluence point of the river marked with high *h(0.80).* A moderate correlation of *Ea*, hypsometric curve head and toe suggests a coupled effect of tectonic uplift and related enhancement of the denudation process in the region.

Conclusion

The Meenachil River, developed mostly in similar lithology, exhibits variation in channel characteristics in the upper catchment region in its longitudinal profile, which is inferred as the influence of tectonic processes. Morphometric and hypsometric parameters of the subwatersheds of the river basin indicate variation in channel characteristics in close spatial proximity, especially by high order subwatersheds (5th and 4th), compared with lower (3rd). Most of the subwatersheds are mature or mature-to-old age stage of geomorphic evolution with a lesser hypsometric integral (*Ea* ≥ 0.30) and concave hypsometric curve. Though the river basin is dominated by fluvial geomorphic processes, the hypsometric curve shape reveals 2 models of landform evolution. Landform evolution is controlled by the fluvial process in Type-1 subwatersheds, having *Ea* < 0.30 and located mostly

in the higher elevation. An earlier stage of the fluvial process followed by later stages of the diffusive process or mass accumulation in the lower catchment region is responsible for landform evolution in Type-IV subwatersheds which are in the mature or mature-to-old age transition stage and with $Ea \geq 0.30$.

Hypsometric curve concavity (*Eh*) and curve head (*h=0.20*) and toe (*h=0.80*) heights augment the concept of spatial variation in the hypsometric characteristics in subwatersheds. High concavity is associated with subwatersheds having a low hypsometric integral, indicating the increased denudation process caused either by fluvial action or the combined fluvial and diffusive process. Among subwatersheds, the 3rd order group has higher concavity and a relatively high hypsometric integral, indicating mass accumulation of the material, derived by fluvial erosion and later stages of deposition, as deducted from the classification of Type-IV hypsometric curves and supported by high hypsometric toe measurements. Spatial heterogeneity in the measured parameters suggests differential response of the Meenachil river basin to tectonic processes, the major NNW-SSE trending lineament running across the study area defining the boundary of spatial variation in the effect of tectonic processes and dividing the basin into 2 segments, showing different landforms and geomorphic evolutional stages. The portion of the watershed above the flow length of 20 km is geomorphologically more active than the section below. The repeated occurrence of seismic events in the proximity confirms neotectonic activity in the region. It can be concluded that the Meenachil river basin, as a single unit, has not reached the steady state equilibrium condition and different land portions respond differently to terrain evolution and ongoing tectonic activity in the region, though lithology is almost analogous.

Acknowledgments

Authors are thankful to the anonymous reviewers for their critical review, constructive comments and suggestions, which improved the quality of the manuscript.

References

Ahmad S., Bhat M.I., Madden C., Bali B.S. (2014). Geomorphic analysis reveals active tectonic deformation on the eastern flank of the Pir Panjal Range, Kashmir Valley, India. Arabian Journal of Geosciences. 7(6):2225-2235. https://doi.org/10.1007/s12517-013-0900-y

Castillo M. (2017). Landscape evolution of the graben of Puerto Vallarta (west-central Mexico) using the analysis of landforms and stream long profiles. Journal South American Earth Science 73: 10-21. https://doi.org/10.1016/j.jsames.2016.11.002

Chattopadhyay S., Kumar S.S., Chattopadhyay, M. (2006). Landscape evolution in parts of Varnanapuram drainage basin, Kerala-a hypsometric approach. Journal Geological Society of India *68*(5): 841-856.

Dash P., Aggarwal S.P., Verma N., Ghosh S. (2014). Investigation of scale dependence and geomorphic stages of evolution through hypsometric analysis: a case study of Sirsa basin, western Himalaya, India. Geocarto International *29*(7): 758-777. https://doi.org/10.1080/10106049.2013.841772

Elias Z.(2013). Quantitative geomorphology of analyzing tectonic activity in the Roczek and Shwork rivers valley in the Zagros Mountains (Iraqi Kurdistan). International Journal of Enhanced Research Science Technology and Engineering 2(11): 22-34.

Gardner T.W. (1983). Experimental study of knickpoint and longitudinal profile evolution in cohesive, homogeneous material. Geological Society of America Bulletin *94*(5): 664-672. https://doi.org/10.1130/0016-7606(1983)94<664:ESOKAL>2.0.CO;2

Gopinath G., Kamalamma A.G., Jesiya N.P., Lemoon K. (2016). Hydro-hypsometric analysis of tropical river basins, Southwest Coast of India using geospatial technology. Journal of Mountain Science *13*(5): 939-946. https://doi.org/10.1007/s11629-015-3589-4

Gopinath G., Swetha T.V., Ashitha M.K. (2014). Elicitation of erosional signature of a tropical river basin with high-resolution stereo data. Applied Geomatics *6*(3): 149-157. ttps://doi.org/10.1007/s12518-014-0127-y

Hancock G.S., Anderson R.S., Whipple K.X. (1998). Beyond power: Bedrock river incision process and form. Rivers over rock: Fluvial processes in bedrock channels 35-60.

Horton R.E. (1945). Erosional development of streams and their drainage basin, Hydro physical approach to quantitative morphology. Geological Society of America Bulletin 56:275–370. https://doi.org/10.1130/0016-7606(1945)56[275:EDOSAT]2.0.CO;2

Hurtrez J.E., Sol C., Lucazeau F. (1999). Effect of drainage area on hypsometry from an analysis of small-scale drainage basins in the Siwalik Hills (Central Nepal). Earth Surface Processes and Landforms 24(9): 799-808. https://doi.org/10.1002/(SICI)1096-9837(199908)24:9<799::AID-ESP12>3.0.CO;2-4

Kale V.S., Shejwalkar N. (2008). Uplift along the western margin of the Deccan Basalt Province: Is there any geomorphometric evidence? Journal of Earth System Science 117(6): 959-971. https://doi.org/10.1007/s12040-008-0081-3

Markose V.J., Jayappa K.S. (2011). Hypsometric analysis of Kali River Basin, Karnataka, India, using geographic information system. Geocarto International *26*(7): 553-568. https://doi.org/10.1080/10106049.2011.608438

Melton M.A. (1957). An analysis of the relation among elements of climate, surface properties and geomorphology. Dept of Geol, Columbia Univ, New York, 102p. https://doi.org/10.21236/AD0148373

Nir D. (1957). The ratio of relative and absolute altitudes of Mt. Carmel, a contribution to the problem of relief analysis and relief classification. Geographical Reviews 47:564–569. https://doi.org/10.2307/211866

Rajendran C.P., John B., Sreekumari K., Rajendran K. (2009). Reassessing the earthquake hazard in Kerala based on the historical and current seismicity. Journal of Geological Society of India. 73: 919–924. https://doi.org/10.1007/s12594-009-0063-3

Singh O., Sarangi A., Sharma M.C. (2008). Hypsometric integral estimation methods and its relevance on erosion status of north-western Lesser Himalayan Watersheds. Water Resources Management 22: 1545-1560. https://doi.org/10.1007/s11269-008-9242-z

Singh N.H., Mathai J., Neelakandan V.N., Shankar D., Singh V.P. (2005). A database on occurrence patterns of unusual geological incidents in Southwest Peninsular India and its implication on future seismic activity. Acta Geodaetica et Geophysica Hungarica *40*(1): 69-8. https://doi.org/10.1556/AGeod.40.2005.1.6

Singh O. (2009). Hypsometry and erosion proneness: a case study in the lesser Himalayan Watersheds. Journal of Soil and Water Conservation *8*(2): 53-59.

Sinha-Roy S. (2002). Hypsometry and landform evolution: a case study in the Banas drainage basin, Rajasthan, with implications for Aravalli uplift. Journal of Geological Society of India *60*(1): 7-26.

Strahler A.N. (1952). Hypsometric (area-altitude) analysis of erosional topography. Geological Society of America Bulletin *63*(11): 1117-1142. https://doi.org/10.1130/0016-7606(1952)63[1117:HAAOET]2.0.CO;2

Strahler A.N. (1956). Quantitative slope analysis. Geological Society of America Bulletin *67*(5): 571-596. https://doi.org/10.1130/0016-7606(1956)67[571:QSA]2.0.CO;2

Trevisani S., Cavalli M., Marchi L. (2010). Reading the bed morphology of a mountain stream: a geomorphometric study on high-resolution topographic data. Hydrology and Earth System Sciences 14:393–405. https://doi.org/10.5194/hess-14-393-2010

Troeh F.R. (1965). Landform equations fitted to contour maps. American Journal of Science *263*(7): 616-627. https://doi.org/10.2475/ajs.263.7.616

Vijith H., Satheesh R. (2006). GIS based morphometric analysis of two major upland sub-watersheds of Meenachil river in Kerala. Journal Indian Society of Remote Senssing *34*(2): 181-185. https://doi.org/10.1007/BF02991823

Vincy M.V., Rajan B., Pradeepkumar A.P. (2012). Geographic information system–based morphometric characterization of sub-watersheds of Meenachil river basin, Kottayam district, Kerala, India. Geocarto International *27*(8): 661-684. https://doi.org/10.1080/10106049.2012.657694

Willgoose G. (1994). A physical explanation for an observed area-slope-elevation relationship for catchments with declining relief. Water Resources Research *30*(2): 151-159. https://doi.org/10.1029/93WR01810

Willgoose G., Hancock G. (1998). Revisiting the hypsometric curve as an indicator of form and process in transport-limited catchment. Earth Surface Processes and Landforms *23*(7): 611-623. https://doi.org/10.1002/(SICI)1096-9837(199807)23:7<611::AID-ESP872>3.0.CO;2-Y

Willgoose G., Bras R.L., Rodriguez-Iturbe I. (1991). A coupled channel network growth and hillslope evolution model: 1. Theory. Water Resources Research *27*(7): 1671-1684. https://doi.org/10.1029/91WR00935

Upės baseino žemės reljefo įvertinimas naudojant hipsometrinę schemą Pietų Vakarų Ghatuose, Indijoje

Gauta:
2017 m. lapkritis
Priimta spaudai:
2017 m. gruodis

H. Vijith
Nepriklausomas mokslininkas, Sarawak, Malaizija

V. Prasannakumar
Geospatial informacijos mokslo ir technologijų centras, Kerala universitetas, Kerala, Indija

P. Pratheesh
Geologijos katedra, Žemės mokslo sistemų mokykla, Centrinis Kerala universitetas, Kerala, Indija

Geomorfinių procesų charakteristikos ir erdviniai variacijos modeliai Meenachil upės baseino Vakarų Ghatose, Keraloje, Analizuojami 49-ojo, 5-osios, 4-osios ir 3-osios pakopų pjūvių hipsometriniai parametrai. Hipsometrinės kreivės ir parametrai, tokie kaip hipsometrinis integralas (Ea), didžiausias įgaubtas (Eh), kreivės įlinkio taško (I) koordinatės (a *, h *) ir hipsometrinės kreivės normalizuoti aukščiai 20%, 50% ir 80% ploto nurodo erdvinius pokyčius. Išilginis upės profilis rodo labai sutrikdytą regioną, virš kurio yra 20 km nuotėkio ir santykinai mažiau sutrikęs plotas pasroviui. Hipomometrinis integralas labiausiai suskirsto į subrendusius ir brandaus amžiaus reljefus, o skirtingos hipsoforminės kreivės formos reiškia tektoninio pakilimo įtaką. Hiposimetrinės išgaubos pokyčiai patvirtina tektoninių procesų poveikį regione, kuriame fluvialio ir difuzinio proceso derinys yra aktyvus ir matomas iš aukšto hipsometrinio pjūvio matavimų. Pasikartojantys žemės drebėjimai regione patvirtina nuolatinę tektoninę veiklą, tiesiogiai susijusią su upių baseino geomorfinėmis savybėmis.

Raktiniai žodžiai: hipsometrija, įgaubtiškumas, krašto formos, hipsometrinės kreivės, hipsometrinis integralas.